Published in final edited form as:
Circ Cardiovasc Imaging. 2011 November ; 4(6): 729–737. doi:10.1161/CIRCIMAGING.111.966374.

Molecular MRI of Acute Necrosis with a Novel DNA-Binding Gadolinium Chelate: Kinetics of Cell Death and Clearance in Infarcted Myocardium:

Huang et al: Molecular MRI of Acute Necrosis

Shuning Huang, PhD[1], **Howard H. Chen, PhD**[1,2], **Hushan Yuan, PhD**[3], **Guangping Dai, PhD**[1], **Daniel T. Schuhle, PhD**[1], **Choukri Mekkaoui, PhD**[1], **Soeun Ngoy**[4], **Ronglih Liao, PhD**[4], **Peter Caravan, PhD**[1], **Lee Josephson, PhD**[1,3], and **David E. Sosnovik, MD**[1,2,5]

[1] Martinos Center for Biomedical Imaging, Department of Radiology, Massachusetts General Hospital, Harvard Medical School

[2] Center for Molecular Imaging Research, Massachusetts General Hospital, Harvard Medical School

[3] Center for Translational Nuclear Medicine and Molecular Imaging, Massachusetts General Hospital, Harvard Medical School

[4] Cardiology Division, Brigham and Woman's Hospital, Harvard Medical School

[5] Cardiology Division, Massachusetts General Hospital, Harvard Medical School

Abstract

Background—Current techniques to image cell death in the myocardium are largely non-specific. Here we report the use of a novel DNA-binding gadolinium chelate (Gd-TO) to specifically detect the exposed DNA in acutely necrotic (ruptured) cells *in vivo*.

Methods and Results—*In vivo* MRI was performed in 20 mice with myocardial infarction (MI). The mice were injected with Gd-TO or Gd-DTPA at varying time points post-MI. MRI was performed 2 hours after probe injection, to avoid nonspecific signal from the late gadolinium enhancement effect. Cell rupture (Gd-TO uptake) was present within 2 hours of infarction, but peaked 9–18 hours after the onset of injury. A significant increase in the longitudinal relaxation rate (R_1) in the infarct was seen in mice injected with Gd-TO within 48 hours of MI, but not in those injected more than 72 hours post MI ($R_1 = 1.24 \pm 0.08$ and 0.92 ± 0.03 s^{-1}, respectively, $p < 0.001$). Gd-DTPA, unlike Gd-TO, washed completely out of acute infarcts within 2 hours of injection ($p < 0.001$). The binding of Gd-TO to exposed DNA in acute infarcts was confirmed with fluorescence microscopy.

Conclusions—Gd-TO specifically binds to acutely necrotic cells and can be used to image the mechanism and chronicity of cell death in injured myocardium. Cell rupture in acute MI begins early but peaks many hours after the onset of injury. The ruptured cells are efficiently cleared by the immune system and are no longer present in the myocardium 72 hours after injury.

Correspondence to: David E. Sosnovik, MD FACC 149 13th Street Charlestown, MA 02129 Tel: 617 724-3407 Fax: 617 726-7422 sosnovik@nmr.mgh.harvard.edu.

Disclosures None.

Keywords

molecular imaging; MRI; necrosis; myocardium; infarction

The transition of cells from a healthy (vital) to an apoptotic or necrotic state is a feature of many cardiovascular diseases including ischemic injury,[1, 2] heart failure,[3] and transplant rejection.[4] Imaging cell death *in vivo* thus has the potential to provide important insights into the pathogenesis and treatment of cardiovascular disease. The imaging of cell death *in vitro* is well established, and fluorescent annexin V (henceforth annexin) and vital fluorochromes such as propidium-iodide are frequently used *in vitro* to image both the kinetics and nature of cell death. Moreover, in a landmark study, this dual fluorochrome approach was used to image cell death in the myocardium of mice *in vivo* using intravital microscopy.[2] In the clinical setting, however, annexin-labeled probes have been used alone as single imaging agents [4, 5]. While of significant value, the information provided solely by annexin imaging does not allow apoptosis and necrosis to be distinguished from each other when both are present. In addition, no translatable imaging strategy has been developed to specifically label necrotic cells, characterize the temporal evolution of necrosis, and image the clearance of necrotic debris from injured myocardium.

To meet these needs, we describe here the development and use of a novel multimodal DNA-binding gadolinium chelate (Gd-TO) to image necrotic cell death *in vivo* by MRI. Gd-TO consists of a gadolinium-chelate, similar to those used clinically, and a DNA-binding vital fluorochrome (TO-PRO 1). Like Gd-DTPA (gadopentetic acid, Magnevist, Schering, Berlin), which was the control probe used in the study, Gd-TO can be imaged *in vivo* 10–30 minutes after injection with delayed enhancement MRI. However, unlike Gd-DTPA, which washes out completely within 40–50 minutes, we hypothesized that Gd-TO would be retained in acutely injured myocardium due to its specific binding to the exposed DNA of acutely necrotic cells. Moreover, we hypothesized that the amount of Gd-TO accumulation would reflect the evolution of necrotic cell death and, subsequently, the clearance of the necrotic cells by the immune system. We further hypothesized that if Gd-TO was injected after the clearance of acutely necrotic cells from the myocardium was completed, that the washout of the agent would be identical to that of Gd-DTPA.

A mouse model of permanent myocardial infarction was used in the study. Gd-TO was injected at various time points following infarction and imaged 2–3 hours after injection, well after the resolution of the non-specific delayed (late) gadolinium enhancement effect. Signal enhancement in the infarct was highest with Gd-TO injections performed 9–18 hours after infarction, was lower following injections in the next 24–48 hours, and no enhancement was seen with Gd-TO injections performed 72–96 hours post injury. The uptake of Gd-TO thus occurred during a narrow time window in which acutely necrotic cells were present within the infarcted myocardium. Using a mouse model of myocardial infarction we thus show that Gd-TO is selectively retained in tissue with acutely necrotic cells, can be used to delineate the time course of cell rupture following injury, and can be used to characterize the rate at which necrotic material is removed from injured tissue.

Gd-TO binds to a molecular target (DNA) common to all necrotic cells and its use is thus relevant in a broad range of cardiovascular diseases. The use of the agent, alone or in combination with other imaging markers, has the potential to provide novel insights into the mechanisms and kinetics of cell death in injured myocardium. Gd-TO is well eliminated and amenable to large-scale synthesis as either a MRI or nuclear imaging agent. A novel molecular imaging approach with broad relevance and significant translational potential is thus presented.

Methods

Simulation and In Vitro Binding Studies

The synthesis of Gd-TO was as described.[6] Briefly, the iodohexyl derivative of thiazole orange was reacted with ethyl 6-N,N'-dimethylaminohexanoate, to afford a linker with a free carboxyl group for chelate attachment. p-NH_2-Bn-DTPA (Macrocyclics, Dallas, TX) was then coupled to the carboxyl group, followed by reaction with gadolinium to yield the gadolinium chelate reporter of Gd-TO. The binding of Gd-TO to DNA was examined by simulation and with *in vitro* assays. Models for the binding of TO-PRO 1 and Gd-TO to DNA were generated based on the experimentally determined NMR structure of a TO bound to complimentary DNA oligonucleotides.[7, 8] Briefly, the MOE 2007.09 docking suite (Chemical Computing Group, Montreal) was used to build 10 base pairs of ideal B-form DNA and energy minimized structures of TO-PRO 1 and GD-TO (MMF94X forcefield to a constant of 0.05 kcal/mol). Due to the predicted solvent exposure of the gadolinium-chelate group and uncertainty in the accuracy of models of this group generated by drug design software, only the linker and amide group of GD-TO were considered. Initial models were generated by superimposing the coordinates for B-form DNA and TO-PRO 1 or GD-TO onto the respective groups in 108D.pdb. Finally, the local interactions between the ligands (GD-TO and TO-PRO 1) and the model DNA were optimized and minimized using the MOE LigX function. This approach is similar to that used previously on similar molecules.

The binding of Gd-TO to DNA and serum albumin was then studied *in vitro*. 35 uM Gd-TO was incubated with calf thymus DNA (0.46 mg/mL, 1380 uM base), bovine serum albumin (40 mg/mL, 69 uM) or phosphate-buffered saline at 37° C for 40 minutes. The filtrate from this incubation was obtained by centrifugation through a 10 kDa cutoff Amicon Ultra filter (Millipore, UFC501024). The concentration of Gd-TO in the filtrate was then determined spectrophotometrically (OD510). A high concentration of Gd-TO in the filtrate indicated minimal binding, while a low concentration indicated strong binding.

Experimental Protocol

The experimental scheme employed is shown in Figure 1. Myocardial infarction was induced in twenty C57Bl6 mice by permanent ligation of the left coronary artery. Five of the infarcted mice were injected with Gd-DTPA (0.1 mmol/kg, ip) 24 –48 hours after infarction (mean 28.8 ± 4.8 hours). The remaining 15 mice were injected with Gd-TO (0.1 mmol/kg, ip) at various time points after myocardial infarction. T_1 weighted MRI scans to detect the presence of gadolinium in the infarct were performed in all mice 2–3 hours after the injection of the imaging agent. This allowed the unbound fraction of both probes to be washed out prior to imaging and ensured that any gadolinium retention would reflect active binding.

MRI was performed on a 9.4 Tesla horizontal bore magnet (Biospec, Bruker, Billerica MA) equipped with a 1500 mT/m gradient insert (Resonance Research Inc, Billerica MA). Prior to T_1 weighted imaging to detect the presence of gadolinium, gradient echo cines were acquired in the short axis of the left ventricle using cardiorespiratory gating (SA Instruments, Stonybrook, NY) and the following settings: Slice 1mm, FOV 25mm × 25mm, Matrix 200 × 200, flip angle 30 degrees, 20 frames per RR interval, TE 1ms, 4 averages. Slices showing wall motion abnormalities on the cine images were deemed to be infarcted and underwent further scanning to detect the presence of gadolinium with an ECG-gated inversion recovery (also known as a modified Look-Locker) sequence (Figure 1).

The ECG-gated inversion recovery sequence consisted of a slice-selective adiabatic 180-degree inversion pulse, which was applied every 3 seconds. Signal along the longitudinal relaxation curve was sampled at multiple inversion times (TI), each defined by a multiple of

the RR interval (Figure 1). It should be noted that the T2 in the myocardium in mice at 9.4 T is approximately 20ms, and thus significantly shorter than the RR interval (approximately 120ms). A spoiled or unspoiled readout can thus be used without T2 contamination of successive images along the inversion recovery curve. At each TI, 4 lines of k-space were acquired with a FISP sequence and the following parameters: FOV 25mm × 25 mm, slice 1mm, matrix 160 × 160, flip angle 20 degrees, TR 3.5 ms, TE 1.38 ms, 4 averages. Maps of the longitudinal relaxation rate (R_1) in the myocardium were constructed offline using Matlab (Mathworks, Natick, MA). Specifically, the apparent longitudinal relaxation rate R_1* was first obtained by fitting the inversion recovery curve, $S(t) = A - Be^{(-t)(R_1*)}$, using a non-linear least square algorithm. The R_1 values were then obtained by modifying the apparent R_1* as previously described,[9] $R_1 = R_1*/[(B/A) - 1]$, for this sequence. The accumulation of Gd-TO or Gd-DTPA in the infarct was quantified by measuring R_1 in those portions of the myocardium showing wall motion abnormalities on cine MRI.

Following MRI, 16/20 of the mice were immediately euthanized and the hearts were embedded and sectioned for fluorescence microscopy. Fluorescence microscopy for Gd-TO was performed on an Olympus IX51 Inverted microscope with the following filters: excitation wavelength 460–490 nm, emission wavelength 510–550. The slides were then stained in-situ with DAPI (Sigma. St Louis, MO) and imaged with the following filters: excitation wavelength 330–385 nm, Emission wavelength 420 nm. Four of the fifteen mice injected with Gd-TO (2 with infarcts less than 48 hours in duration, and 2 with infarcts greater than 72 hours in duration) were euthanized 24 hours after the Gd-TO injection (21 hours after the MRI) for inductively coupled plasma mass spectrometry (ICP-MS) of gadolinium biodistribution. ICP-MS for gadolinium was performed in the blood, heart, lungs, brain, kidney, liver, spleen, bone, stomach, pancreas and intestines. All samples were digested in 70% nitric acid overnight at 40°C. A dysprosium solution was added as an internal standard to correct for any evaporative loss. Each digest was then diluted into a 5% nitric acid solution containing lutetium as an internal standard. Metal ions were assayed using an Agilant 7500 Series ICP-MS, and the gadolinium concentration was determined by comparing the Gd:Lu count ratio in each sample to a standard curve. Each digest was measured in duplicate. Gadolinium content in each organ was calculated as percentage injected dose (%ID) per organ and %ID per gram.

The uptake of Gd-TO by activated macrophages was also studied. Activated macrophages were obtained via peritoneal lavage in a mouse model of thioglycollate-induced peritonitis. The activated macrophages were exposed to 1uM of Gd-TO at 37° C for 15 minutes. A second group of activated macrophages was exposed to Gd-TO after their cell membranes had been permeabilized with a surfactant (Cytofix/Cytoperm Fixation/Permeabilization kit, Becton-Dickinson, Franklin Lakes, NJ). Gd-TO uptake in the two groups of cells was assessed with flow cytometry (4 Laser LSR II, Becton-Dickinson). In addition, fluorescence microscopy for Gd-TO and DAPI in the two cell populations was performed as described above.

Statistical analysis of the data was performed with Prism (Graphpad, La Jolla Ca). Comparisons between more than 2 groups were performed with an ANOVA test and a Tukey's post-test comparison. Values throughout the paper are expressed as mean ± standard error and a p-value of < 0.05 was required to meet significance. All animal studies described in the paper were conducted in accordance with the policies for research animal use at our institution, and with the approval of the subcommittee for research animal use at our institution.

Results

The essential features of Gd-TO, its structure, binding to DNA and lack of albumin binding, are shown in Figure 2. Gd-TO's design (Figure 2) is based on the precursor structure TO-PRO 1 (Figure 2 A–B), which is a membrane impermeable vital dye.[6, 10] The quaternary nitrogen on TO-PRO 1 provides a permanent positive charge that likely prevents its entry into healthy (vital) cells. Gd-TO's design (Figure 2C) preserves the rings of TO, and the quaternary nitrogen of TO-PRO 1, while adding a six-carbon carboxyl group terminated linker (red) and chelated Gd reporter (green). The results of our simulation studies revealed that the attachment of a Gd chelate to TO-PRO 1 did not change its binding to DNA. The rings of TO-PRO 1 (Figure 2D) and Gd-TO (Figure 2E) intercalated similarly into double stranded DNA (arrows), while their quaternary amines formed electrostatic bonds (dotted rectangles) with the phosphate groups of DNA. Our model indicates that when Gd-TO binds DNA, its six-carbon linker swings out from the double helix and is unlikely to affect binding.

In vitro binding assays confirmed the affinity of Gd-TO for DNA. Incubation of Gd-TO (35 uM) with DNA (1360 uM base) resulted in profound retention of the agent and the absence of Gd-TO in the filtrate (Figure 2F). In contrast, both albumin (69 uM) and phosphate-buffered saline failed to bind Gd-TO, yielding a filtrate that contained the full concentration of Gd-TO. The failure of Gd-TO to bind albumin is noteworthy given the affinity of many other fluorochromes (e.g. indocyanine green, bromocresol green, cibacron blue) for serum albumin.

Representative images of an infarcted mouse, injected with Gd-TO 6h after infarction (imaged 9h after infarction) are shown in Figure 3. At the nth heartbeat after the inversion pulse (Figure 3A, RR(n)), the infarcted myocardium has reached the null point (NP) and appears dark, while the blood pool (BP) and uninjured septum (white arrow) have slower relaxation rates and have not yet reached the NP. Two heartbeats later, (Figure 3B, RR (n +2)), the signal in the blood pool and non-infarcted septum are nulled, while the infarct has passed through the NP and appears bright (yellow arrows). A further 2 heartbeats later (Figure 3C, RR(n+4)), all signals have passed through the NP. However, the uptake Gd-TO has increased the longitudinal relaxation (R_1) in the infarct, which thus appears hyperintense (bright) relative to the uninfarcted septum.

Profound uptake of Gd-TO was seen in infarcted mice injected with the agent within 48 hours of infarction (n=9). This can be seen in a frame from the inversion recovery sequence (Figure 4A), where the septum and blood pool are nulled relative to the hyperintense infarct, and by the significant increase in R_1 in the infarct (Figure 4B). In contrast, no retention of gadolinium or increase in R_1 was seen in mice with acute infarcts that were injected with Gd-DTPA (Figure 4 C–D). Likewise, no increase in R_1 was seen in mice with infarcts older than 72–96 hours injected with Gd-TO (n=6). Thus, Gd-TO was retained only in recently infarcted myocardium, while Gd-DTPA had no effect on signal intensity or R_1 due to its complete washout in the 2–3 hour period between injection and imaging.

The uptake of Gd-TO (R_1) as a function of infarct evolution (time post coronary ligation) is shown in Figure 5. Within 2–3 hours of infarction a statistically significant increase in R_1 was seen in mice injected with Gd-TO versus those mice with acute infarcts injected with Gd-DTPA (0.98 ± 0.1 versus 0.76 ± 0.02 s^{-1}, $p < 0.05$ with both unpaired t-test and Mann-Whitney). This suggests that cell rupture and DNA exposure in myocardial infarction begins to occur within 2 hours of injury. The increase in infarct R_1 with Gd-TO was highest in those mice injected 9–18 hours after infarction and declined in those mice injected at later time points. No signs of Gd-TO accumulation were seen in those mice injected more than

72–96 hours after infarction. Kinetic fitting of the R_1 curve (Figure 5B) showed that it could be well fitted using a three-compartment model in which cardiomyocytes transition from a healthy to a necrotic state, and are then cleared. Each transition process is governed by a different rate constant. A time delay of 18 hours from the onset of injury to the onset of necrotic cell clearance produced the optimal fit. A mathematical description of the model used to fit the data is provided in the data supplement.

Additional analysis (ANOVA) was performed with the mice divided into the following three groups (Figure 5C): Those injected with Gd-DTPA within 24–48 hours of infarction (mean time 28.8 ± 4.8 hours), those injected with Gd-TO less than 48 hours from the onset of infarction, and those injected with Gd-TO 72 hours or more after infarction. Significant differences were seen in the R_1 of those mice injected with Gd-TO less than 48 hours from infarction and those injected with Gd-TO 72 hours or more after infarction (1.24 ± 0.08 versus 0.92 ± 0.03 s^{-1}, $p < 0.001$). Likewise significant differences were present in the mice injected with Gd-TO within 48 hours of infarction and those injected within 24–48 hours of infarction with Gd-DTPA (1.24 ± 0.08 versus 0.76 ± 0.02 s^{-1}, $p < 0.001$).

No evidence of Gd-TO accumulation was seen either by MRI or fluorescence microscopy in non-infarcted myocardium. However, in those mice imaged within 48 hours of infarction, large amounts of Gd-TO were seen within the infarct. Patchy uptake of Gd-TO was also seen in these mice in the infarct border zone, consistent with the presence of normal and necrotic cells in this region. An excellent degree of co-localization was seen between Gd-TO and a DAPI (nuclear) co-stain, confirming that GD-TO was bound to the nuclei of necrotic cells. These findings are well demonstrated in the fluorescence microscopy images of a mouse injected with Gd-TO and imaged 18 hours after myocardial infarction (Figure 6 A–D). Flow cytometry of the activated macrophages (Figure 6E) revealed that Gd-TO was taken up by these cells only once their cell membranes had been permeabilized. Gd-TO accumulation in the permeabilized macrophages co-localized very strongly with DAPI staining (Figure 6 F–H). Gd content, determined by ICP-MS in 4 mice 24 hours after the injection of Gd-TO, is shown the Table. Overall, less than 4% of the injected Gd remained in the body 24 hours after injection.

Discussion

The central role of cell death in cardiovascular disease makes the detailed understanding of this process imperative.[11, 12] We present here a novel DNA-binding agent, Gd-TO, to image necrotic cell death *in vivo* by MRI. The specificity of Gd-TO for acute necrotic cell death is demonstrated in a mouse model of myocardial infarction. We show that the agent has the unique ability to image both the mechanism and chronicity of cell death through a novel and well-elucidated molecular mechanism. While we focus in the current study on a mouse model of myocardial infarction, the utility of the agent is extremely broad and it can be used to image necrotic cell death in any cardiovascular condition. A versatile, well-characterized and effective platform for the imaging of acute necrotic cell death is thus presented.

The kinetics and mechanisms of cell death in the myocardium, remain incompletely understood.[12, 13] Moreover, the response of serological biomarkers such as troponin to injury within a solid organ can be highly delayed and nonlinear.[14] In contrast, the use of a vital imaging agent such as Gd-TO provides a direct and spatially resolved readout of cell death at the local level. Gd-TO uptake in this study was present within 2 hours of myocardial infarction and peaked between 9–18 hours of injury. This suggests that cell rupture and significant changes in membrane permeability begin within 1–2 hours of infarction. Full disintegration and rupture of the cell, however, takes many more hours to occur and maximal uptake of Gd-TO thus occurred 9–18 hours after infarction. This time

course is consistent with previous histological data using an antimyosin antibody.[15] Notwithstanding differences in human and murine pathophysiology, the kinetics of Gd-TO accumulation provide valuable insights into the kinetics of serological biomarkers such as troponin. Troponin elevation in patients with acute coronary syndromes is frequently detected only 6–12 hours after injury,[14] well after the initial uptake of Gd-TO in this study. This suggests that the release of troponin into the extracellular space is a late event in cardiomyocyte necrosis, and that elevations in serum troponin will be seen only once profound disintegration of the cardiomyocyte membrane has occurred.

The response of the inflammatory system to the release of cellular DNA has been extensively studied.[16, 17] Free DNA in its own right serves as a danger signal, stimulating an inflammatory response.[16] DNA also interacts with toll-like receptors on monocytes,[18] promoting phagocytosis. In addition, several opsonins that bind DNA and promote its phacocytosis have been identified including C1q,[19] mannose-binding lectin,[20] ficolin-2 and 3,[21] properdin,[22] and histidine-rich glycoprotein.[23] These and other mechanisms result in a robust monocyte infiltrate within the infarct, which in mice reaches full threshold approximately 24 hours after injury.[24, 25] The absence of Gd-TO uptake 72–96 hours after myocardial infarction suggests that the removal of necrotic cell debris by infiltrating monocytes is completed within 2–3 days, consistent with prior histological studies.[24] Interestingly, this time point corresponds to the transition of the monocytes infiltrating infarcted myocardium from highly degradative lys6C-high monocytes to more reparative lys6C-low monocytes.[25]

Antibodies targeted to specific antigens, such as myosin,[26] can be used to image membrane integrity. However, antibodies are far too large for renal elimination and frequently show high non-specific hepatic accumulation. The simultaneous use of radiolabeled annexin and anti-myosin antibodies,[27, 28] although of value, is thus significantly limited by these factors. In contrast, the molecular weights of TO and the complete Gd-TO molecule are 305 Da and 1110 Da, respectively. Gd-TO's physical properties (small size, water solubility, lack of albumin binding) likely contribute to its rapid clearance from the blood and its low tissue retention at 24 hours (Table), a prerequisite for the clinical translation of any gadolinium-based agent. Imaging of Gd-TO uptake was performed 2–3 hours after injection in this proof-of-principle study. However, images acquired in our study one hour after injection suggest that this time point would also be highly suitable for the imaging of Gd-TO.

The development of T_2 weighted MRI sequences to image tissue edema has been a major advance.[29, 30] However, T_2 hyperintensity is a non-specific signature, and cannot differentiate acute (less than 72 hours) from subacute (less than 6 weeks) injury. The use of serological biomarkers such as troponin is frequently helpful, but not definitive, in these situations. Regions of acute and subacute injury, for instance, can frequently co-exist and cannot be easily distinguished from each other using T_2 weighted MRI and serological biomarkers. The availability of a single definitive imaging test to differentiate acute from subacute injury would thus be a valuable advance. Moreover, the use of Gd-TO to study the mechanism, kinetics and immune response to cell death has the potential to yield valuable insights into myocardial injury and result in improved therapeutic strategies.

Delayed (late) enhancement imaging of extracellular chelates in the myocardium is based on changes in the extracellular volume of distribution of the chelate, and is a non-specific finding seen in both acute and chronic injury.[31, 32] Gadolinium chelates such as gadoporphyrin, which preferentially accumulate in necrotic tissue have been developed.[33, 34] However, the mechanism of uptake of these agents is completely non-specific and is likely related to binding to a variety of proteins and connective tissue elements. In contrast, the uptake of Gd-TO occurs via a specific and well-elucidated molecular mechanism and is thus

able to provide novel insights into the kinetics of cell death and clearance in infarcted myocardium.

Molecular MRI of apoptosis *in vivo* has been performed with several constructs, most notably the superparamagnetic nanoparticle AnxCLIO-Cy5.5. In an initial proof-of-principle study in the heart, this agent was used alone and was thus not able to distinguish apoptosis from necrosis.[35] In a subsequent study, delayed enhancement of gadolinium (Gd-DTPA) was used in conjunction with AnxCLIO-Cy5.5 to attempt to resolve the various forms of cell death in the myocardium.[36] While of value, the non-specific nature and limitations of delayed enhancement imaging have been discussed above. The availability of AnxCLIO-Cy5.5 and Gd-TO now makes it possible to replicate, in the *in vivo* setting, the robust dual fluorochrome approach used during intravital microscopy and flow cytometry.

In conclusion, the work presented here is, to the best of our knowledge, the first demonstration of molecular MRI with a multimodal vital imaging agent. We show that Gd-TO is able to image the mechanism of cell death as well as the evolution and clearance of necrotic cells in acute ischemia. In addition, we show that inflammatory cells do not take up Gd-TO, making the agent suitable for imaging necrotic cell death in highly inflammatory milieus such as infarcted myocardium, myocarditis and transplant rejection. Gd-TO does not require the synthesis of new biological materials and is well suited to synthesis at the scale needed for large animal and human studies. The structure, binding and mechanism of uptake of Gd-TO are all well understood, and it is well eliminated. The potential of Gd-TO, or a radioactive TO analogue, to undergo successful clinical translation is thus high.

Supplementary Material

Refer to Web version on PubMed Central for supplementary material.

Acknowledgments

We thank Galen Loving and Yan Yang for their assistance with the ICP-MS measurements. We thank Kristopher Josephson for his assistance in the modeling of Gd-TO binding to DNA.

Sources of Funding Funded by the following National Institutes of Health grants: R01 HL093038 (DES), R01 EB011996 (LJ), S10RR025563 (GD) and P41RR14075 (Martinos Center).

References

1. Gottlieb RA, Burleson KO, Kloner RA, Babior BM, Engler RL. Reperfusion injury induces apoptosis in rabbit cardiomyocytes. J Clin Invest. 1994; 94:1621–1628. [PubMed: 7929838]
2. Dumont EA, Reutelingsperger CP, Smits JF, Daemen MJ, Doevendans PA, Wellens HJ, Hofstra L. Real-time imaging of apoptotic cell-membrane changes at the single-cell level in the beating murine heart. Nat Med. 2001; 7:1352–1355. [PubMed: 11726977]
3. Hayakawa Y, Chandra M, Miao W, Shirani J, Brown JH, Dorn GW 2nd, Armstrong RC, Kitsis RN. Inhibition of cardiac myocyte apoptosis improves cardiac function and abolishes mortality in the peripartum cardiomyopathy of Galpha(q) transgenic mice. Circulation. 2003; 108:3036–3041. [PubMed: 14638549]
4. Narula J, Acio ER, Narula N, Samuels LE, Fyfe B, Wood D, Fitzpatrick JM, Raghunath PN, Tomaszewski JE, Kelly C, Steinmetz N, Green A, Tait JF, Leppo J, Blankenberg FG, Jain D, Strauss HW. Annexin-V imaging for noninvasive detection of cardiac allograft rejection. Nat Med. 2001; 7:1347–1352. [PubMed: 11726976]
5. Hofstra L, Liem IH, Dumont EA, Boersma HH, van Heerde WL, Doevendans PA, De Muinck E, Wellens HJ, Kemerink GJ, Reutelingsperger CP, Heidendal GA. Visualisation of cell death in vivo in patients with acute myocardial infarction. Lancet. 2000; 356:209–212. [PubMed: 10963199]

6. Garanger E, Hilderbrand SA, Blois JT, Sosnovik DE, Weissleder R, Josephson L. A DNA-binding Gd chelate for the detection of cell death by MRI. Chem Commun (Camb). 2009:4444–4446. [PubMed: 19597620]
7. Prodhomme S, Demaret JP, Vinogradov S, Asseline U, Morin-Allory L, Vigny P. A theoretical and experimental study of two thiazole orange derivatives with single- and double-stranded oligonucleotides, polydeoxyribonucleotides and DNA. J Photochem Photobiol B. 1999; 53:60–69. [PubMed: 10672530]
8. Spielmann HP, Wemmer DE, Jacobsen JP. Solution structure of a DNA complex with the fluorescent bis-intercalator TOTO determined by NMR spectroscopy. Biochemistry. 1995; 34:8542–8553. [PubMed: 7612596]
9. Messroghli DR, Radjenovic A, Kozerke S, Higgins DM, Sivananthan MU, Ridgway JP. Modified Look-Locker inversion recovery (MOLLI) for high-resolution T1 mapping of the heart. Magn Reson Med. 2004; 52:141–146. [PubMed: 15236377]
10. Van Hooijdonk CA, Glade CP, Van Erp PE. TO-PRO-3 iodide: a novel HeNe laser-excitable DNA stain as an alternative for propidium iodide in multiparameter flow cytometry. Cytometry. 1994; 17:185–189. [PubMed: 7530620]
11. Hotchkiss RS, Strasser A, McDunn JE, Swanson PE. Cell death. N Engl J Med. 2009; 361:1570–1583. [PubMed: 19828534]
12. Whelan RS, Kaplinskiy V, Kitsis RN. Cell death in the pathogenesis of heart disease: mechanisms and significance. Annu Rev Physiol. 2010; 72:19–44. [PubMed: 20148665]
13. Kostin S, Pool L, Elsasser A, Hein S, Drexler HC, Arnon E, Hayakawa Y, Zimmermann R, Bauer E, Klovekorn WP, Schaper J. Myocytes die by multiple mechanisms in failing human hearts. Circ Res. 2003; 92:715–724. [PubMed: 12649263]
14. Lewis GD, Wei R, Liu E, Yang E, Shi X, Martinovic M, Farrell L, Asnani A, Cyrille M, Ramanathan A, Shaham O, Berriz G, Lowry PA, Palacios IF, Tasan M, Roth FP, Min J, Baumgartner C, Keshishian H, Addona T, Mootha VK, Rosenzweig A, Carr SA, Fifer MA, Sabatine MS, Gerszten RE. Metabolite profiling of blood from individuals undergoing planned myocardial infarction reveals early markers of myocardial injury. J Clin Invest. 2008; 118:3503–3512. [PubMed: 18769631]
15. Kajstura J, Cheng W, Reiss K, Clark WA, Sonnenblick EH, Krajewski S, Reed JC, Olivetti G, Anversa P. Apoptotic and necrotic myocyte cell deaths are independent contributing variables of infarct size in rats. Lab Invest. 1996; 74:86–107. [PubMed: 8569201]
16. Kono H, Rock KL. How dying cells alert the immune system to danger. Nat Rev Immunol. 2008; 8:279–289. [PubMed: 18340345]
17. Poon IK, Hulett MD, Parish CR. Molecular mechanisms of late apoptotic/necrotic cell clearance. Cell Death Differ. 2010; 17:381–397. [PubMed: 20019744]
18. Marshak-Rothstein A. Toll-like receptors in systemic autoimmune disease. Nat Rev Immunol. 2006; 6:823–835. [PubMed: 17063184]
19. Gaipl US, Kuenkele S, Voll RE, Beyer TD, Kolowos W, Heyder P, Kalden JR, Herrmann M. Complement binding is an early feature of necrotic and a rather late event during apoptotic cell death. Cell Death Differ. 2001; 8:327–334. [PubMed: 11550084]
20. Nauta AJ, Raaschou-Jensen N, Roos A, Daha MR, Madsen HO, Borrias-Essers MC, Ryder LP, Koch C, Garred P. Mannose-binding lectin engagement with late apoptotic and necrotic cells. Eur J Immunol. 2003; 33:2853–2863. [PubMed: 14515269]
21. Jensen ML, Honore C, Hummelshoj T, Hansen BE, Madsen HO, Garred P. Ficolin-2 recognizes DNA and participates in the clearance of dying host cells. Mol Immunol. 2007; 44:856–865. [PubMed: 16730064]
22. Xu W, Berger SP, Trouw LA, de Boer HC, Schlagwein N, Mutsaers C, Daha MR, van Kooten C. Properdin binds to late apoptotic and necrotic cells independently of C3b and regulates alternative pathway complement activation. J Immunol. 2008; 180:7613–7621. [PubMed: 18490764]
23. Jones AL, Poon IK, Hulett MD, Parish CR. Histidine-rich glycoprotein specifically binds to necrotic cells via its amino-terminal domain and facilitates necrotic cell phagocytosis. J Biol Chem. 2005; 280:35733–35741. [PubMed: 16107330]

24. Dewald O, Ren G, Duerr GD, Zoerlein M, Klemm C, Gersch C, Tincey S, Michael LH, Entman ML, Frangogiannis NG. Of mice and dogs: species-specific differences in the inflammatory response following myocardial infarction. Am J Pathol. 2004; 164:665–677. [PubMed: 14742270]
25. Nahrendorf M, Swirski FK, Aikawa E, Stangenberg L, Wurdinger T, Figueiredo JL, Libby P, Weissleder R, Pittet MJ. The healing myocardium sequentially mobilizes two monocyte subsets with divergent and complementary functions. J Exp Med. 2007; 204:3037–3047. [PubMed: 18025128]
26. Khaw BA, Gold HK, Yasuda T, Leinbach RC, Kanke M, Fallon JT, Barlai-Kovach M, Strauss HW, Sheehan F, Haber E. Scintigraphic quantification of myocardial necrosis in patients after intravenous injection of myosin-specific antibody. Circulation. 1986; 74:501–508. [PubMed: 3017604]
27. Sarda-Mantel L, Hervatin F, Michel JB, Louedec L, Martet G, Rouzet F, Lebtahi R, Merlet P, Khaw BA, Le Guludec D. Myocardial uptake of 99mTc-annexin-V and 111Inantimyosin-antibodies after ischemia-reperfusion in rats. Eur J Nucl Med Mol Imaging. 2008; 35:158–165. [PubMed: 17805532]
28. Sarda-Mantel L, Michel JB, Rouzet F, Martet G, Louedec L, Vanderheyden JL, Hervatin F, Raguin O, Vrigneaud JM, Khaw BA, Le Guludec D. (99m)Tc-annexin V and (111)Inantimyosin antibody uptake in experimental myocardial infarction in rats. Eur J Nucl Med Mol Imaging. 2006; 33:239–245. [PubMed: 16283183]
29. Abdel-Aty H, Cocker M, Meek C, Tyberg JV, Friedrich MG. Edema as a very early marker for acute myocardial ischemia: a cardiovascular magnetic resonance study. J Am Coll Cardiol. 2009; 53:1194–1201. [PubMed: 19341860]
30. Berry C, Kellman P, Mancini C, Chen MY, Bandettini WP, Lowrey T, Hsu LY, Aletras AH, Arai AE. Magnetic resonance imaging delineates the ischemic area at risk and myocardial salvage in patients with acute myocardial infarction. Circ Cardiovasc Imaging. 2010; 3:527–535. [PubMed: 20631034]
31. Kim RJ, Wu E, Rafael A, Chen EL, Parker MA, Simonetti O, Klocke FJ, Bonow RO, Judd RM. The use of contrast-enhanced magnetic resonance imaging to identify reversible myocardial dysfunction. N Engl J Med. 2000; 343:1445–1453. [PubMed: 11078769]
32. Gerber BL, Belge B, Legros GJ, Lim P, Poncelet A, Pasquet A, Gisellu G, Coche E, Vanoverschelde JL. Characterization of acute and chronic myocardial infarcts by multidetector computed tomography: comparison with contrast-enhanced magnetic resonance. Circulation. 2006; 113:823–833. [PubMed: 16461822]
33. Lee SS, Goo HW, Park SB, Lim CH, Gong G, Seo JB, Lim TH. MR imaging of reperfused myocardial infarction: comparison of necrosis-specific and intravascular contrast agents in a cat model. Radiology. 2003; 226:739–747. [PubMed: 12601203]
34. Marchal G, Ni Y, Herijgers P, Flameng W, Petre C, Bosmans H, Yu J, Ebert W, Hilger CS, Pfefferer D, Semmler W, Baert AL. Paramagnetic metalloporphyrins: infarct avid contrast agents for diagnosis of acute myocardial infarction by MRI. Eur Radiol. 1996; 6:2–8. [PubMed: 8797942]
35. Sosnovik DE, Schellenberger EA, Nahrendorf M, Novikov MS, Matsui T, Dai G, Reynolds F, Grazette L, Rosenzweig A, Weissleder R, Josephson L. Magnetic resonance imaging of cardiomyocyte apoptosis with a novel magneto-optical nanoparticle. Magn Reson Med. 2005; 54:718–724. [PubMed: 16086367]
36. Sosnovik DE, Garanger E, Aikawa E, Nahrendorf M, Figuiredo JL, Dai G, Reynolds F, Rosenzweig A, Weissleder R, Josephson L. Molecular MRI of cardiomyocyte apoptosis with simultaneous delayed-enhancement MRI distinguishes apoptotic and necrotic myocytes in vivo: potential for midmyocardial salvage in acute ischemia. Circ Cardiovasc Imaging. 2009; 2:460–467. [PubMed: 19920044]

Clinical Perspective

Necrotic cell death can be detected in vitro with DNA-binding vital fluorochromes such as propidium-iodide. Here we present Gd-TO, a DNA-binding gadolinium (Gd) chelate for the specific imaging of necrotic cell death by MRI in vivo. Gd-TO consists of a Gd chelate conjugated to the DNA-binding vital dye TOPRO-1. We show, in a mouse model of myocardial infarction (MI), that Gd-TO robustly images acute necrotic cell death in vivo. While uptake of Gd-TO was seen within 2 hours of infarction, peak uptake occurred 9–18 hours post-MI. This pattern parallels the release of troponin by cardiomyocytes (CMs) and suggests that CM rupture peaks many hours after the onset of myocardial ischemia. No uptake of Gd-TO was seen in mice injected with the agent more than 72 hours post-MI. This suggests that necrotic cells are rapidly and efficiently cleared from the myocardium within 72 hours of injury. Gd-TO provides a readout that is specific for acute (< 72 hours) necrotic cell death and can be used to assess the kinetics, mechanism (apoptosis versus necrosis) and chronicity of cell death in vivo. Current techniques such as delayed enhancement and T2-weighted MR imaging, while of major value, are not specific for cell death and may not be able to differentiate acute (< 72 hours) from subacute (< 30 days) injury. Gd-TO thus has the potential to become a useful clinical tool and play an important role in the diagnosis and characterization of cell death.

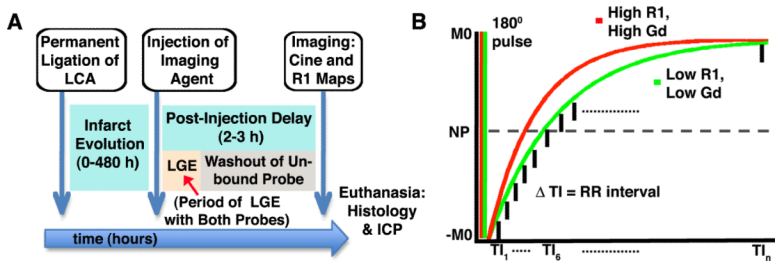

Figure 1.

(A) Experimental protocol: Myocardial infarcts were allowed to evolve for 0–480 hours before the imaging agent (Gd-TO or Gd-DTPA) was injected. Late gadolinium enhancement (LGE) due to slow washout in the infarct is seen with both of probes for 30–40 minutes post-injection. MRI was therefore performed 2–3 hours after the injection of the imaging agent to allow complete resolution of the LGE effect and the washout of any unbound probe. (B) An ECG-gated inversion recovery imaging sequence was used to measure the longitudinal magnetic relaxation rate R1 (sec-1) in infarcted myocardium. The inverted magnetization (−M0) recovers towards its baseline state (M0) with the rate constant R1. Tissues with high Gd concentrations have a higher R1 and thus a steeper recovery curve. NP = null point, TI = inversion time.

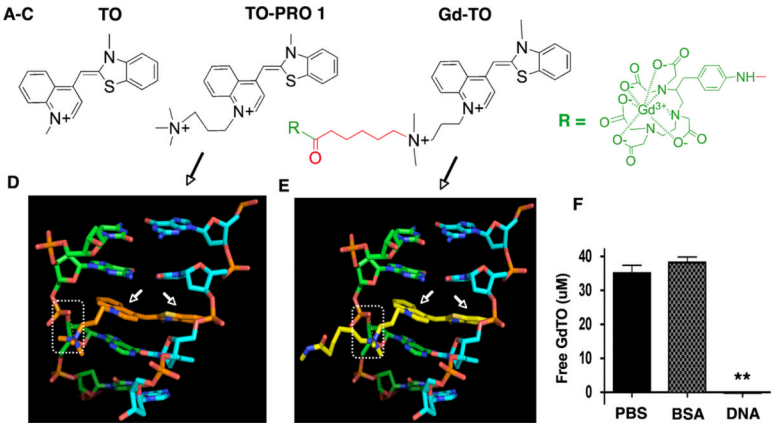

Figure 2.

Structure of Gd-TO and its interaction with DNA. (A–C) From left to right, the structures of thiazole orange (TO), TO-PRO 1 and Gd-TO are shown. TO-PRO 1 and Gd-TO feature quaternary nitrogens, rendering them membrane impermeable. The design of Gd-TO is based on TO-PRO 1, with a quaternary amine, a carboxy terminated linker (red), and a pNH2-Bn-DTPA:Gd chelate reporter (green). (D) The intercalation of the TO-PRO-1 (orange structure, white arrows) with double stranded DNA is compared with (E) the intercalation of Gd-TO (yellow structure, white arrows) with DNA. The quaternary nitrogens on the aliphatic arms of both compounds form salt bridges (dashed rectangles) with the phosphate groups of DNA. (F) Filtration assay showing binding of Gd-TO to DNA but not to albumin (BSA). Gd-TO was incubated with DNA or BSA and the level of free unbound Gd-TO was determined in the filtrate. DNA bound and retained Gd-TO, while BSA and the PBS control did not. ** ($p < 0.001$).

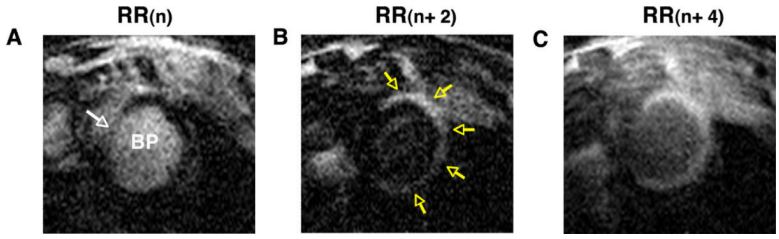

Figure 3.

Gd-TO uptake in an infarcted mouse, imaged 9 hours after LCA ligation. Three frames of an ECG-gated inversion recovery sequence are shown, each separated by 2 RR intervals (heartbeats). (A) At the inversion time (TI) of RR(n) the signal in the infarcted myocardium has reached the null point (NP) and appears dark. The signals in the blood pool (BP) and septum (white arrow) have slower relaxation rates and have not yet reached the NP. (B) At RR (n+2) the signals in the BP and septum are nulled, while the infarct has passed through the NP and appears bright (yellow arrows). (C) At RR(n+4) all signals have passed through the NP. However, the high content of Gd-TO in the infarct has produced a greater degree of longitudinal relaxation and the infarct thus appears hyperintense.

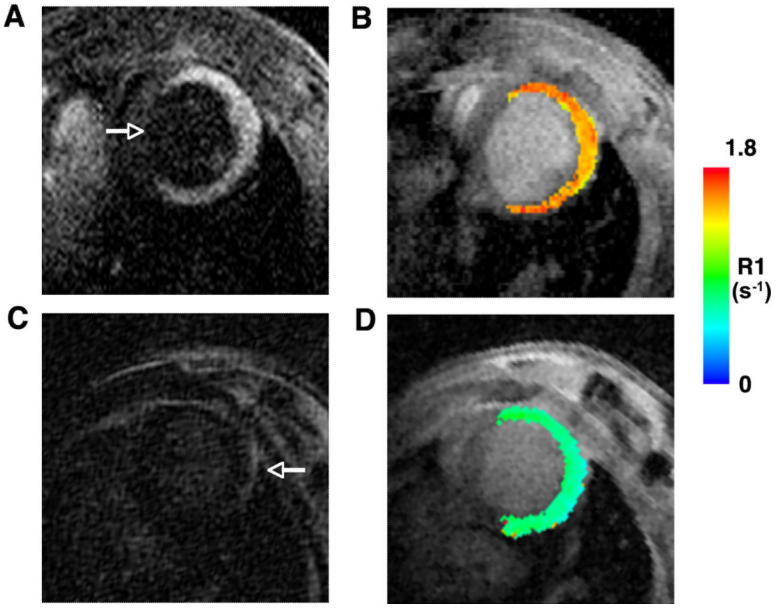

Figure 4.

Comparison of MR images in mice with acute myocardial infarcts injected with either Gd-TO (A, B) or Gd-DTPA (C, D). The mice shown were imaged 18–24 hours after infarction. Both mice showed severe wall motion abnormalities in their anterior, lateral and inferior walls, consistent with extensive infarcts. The arrow in panel (A) points to the uninjured septum. (A, B) Robust accumulation of Gd-TO is seen in the infarct 2–3 hours after injection, producing signal hyperintensity and high R1 values. (C) In contrast 2–3 hours after the injection of Gd-DTPA there is no sign of an increase in signal intensity in the infarct, which is nulled and isointense with the septum. The arrow in panel (C) points to the pericardial fat, which marks the outer border of the infarcted myocardium. (D) A R1 map of the mouse injected with Gd-DTPA shows no increase in R1. Thus Gd-TO is retained in acute myocardial infarcts, while GD-DTPA is not.

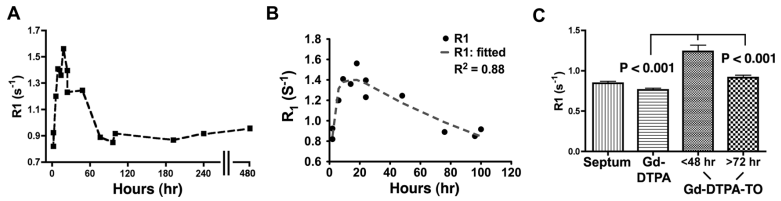

Figure 5.

Ability of Gd-TO to distinguish acutely necrotic myocardium. (A) The time course of Gd-TO accumulation was determined as the R1 of the infarcted myocardium. No uptake of the agent is seen 72–96 hours after infarction. (B) The uptake of Gd-TO can be well fitted using a three-compartment model in which cardiomyocytes move from a healthy to a necrotic state, and are then cleared. Each transition is governed by a different rate constant. A time delay of 18 hours from the initial injury to the onset of necrotic cell clearance produced the optimal fit. (C) R1 values for the uninjured septum, acutely infarcted mice injected with Gd-DTPA, and infarcted mice injected with Gd-TO are shown. Gd-TO uptake distinguished infarcts with evolution times of less than 48 hours from those with durations of greater than 72 hours ($p < 0.001$). Likewise, significant differences ($p < 0.001$) in myocardial R1 were seen between mice with acute infarcts (< 48 hours) injected with Gd-TO and those injected with Gd-DTPA. The accumulation of Gd-TO thus specifically identifies acutely necrotic cells.

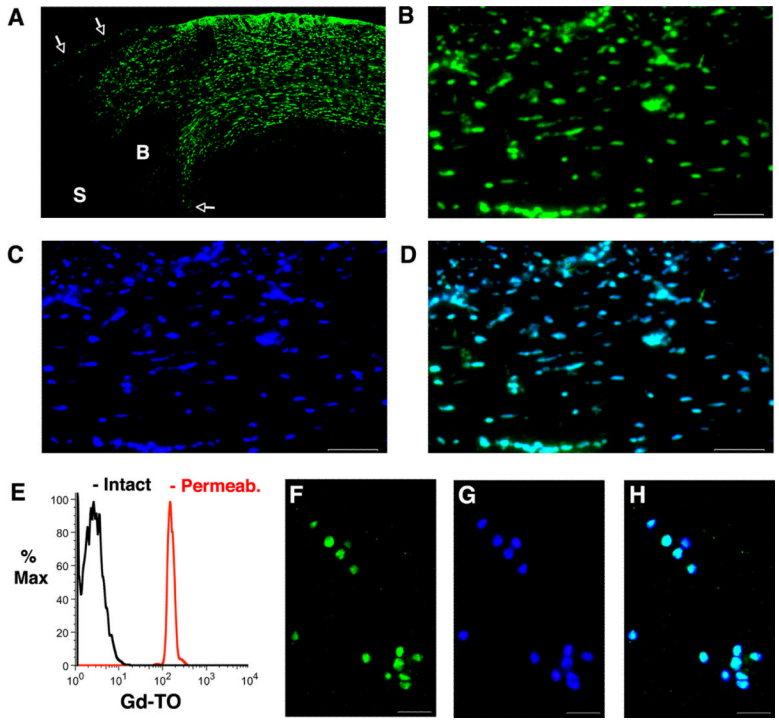

Figure 6.

Fluorescence microscopy of Gd-TO in a mouse imaged 18 hours after myocardial infarction. (A) Low magnification (4×) view of the infarct, border zone and uninjured septum. The white arrows mark the endocardial and epicardial borders of the myocardium. S = Septum, B = Border zone. Extensive amounts of Gd-TO (green channel) are seen in the thinned infarct. The border zone contains areas of normal myocardium interspersed with areas showing Gd-TO uptake. No accumulation of Gd-TO is seen in the uninjured septum. (B) High magnification (20×) view of Gd-TO accumulation (green channel) in the infarct. (C) Identical section to that shown in panel B, after nuclear staining with DAPI. (D) Fusion of the Gd-TO (B) and DAPI (C) images. Gd-TO co-localizes very strongly with DAPI, a nuclear stain, but only in areas of infarction. Scale bar = 100 um. (E–H) Flow cytometry and microscopy of activated macrophages exposed to Gd-TO. (E) Flow cytometry reveals that Gd-TO is not taken up by activated macrophages (black curve). Permeabilization of their membranes by exposure to a surfactant, however, results in significant accumulation of Gd-TO (red curve). Fluorescence microscopy of activated macrophages after permeabilization confirms the uptake and strong co-localization of (F) Gd-TO and (G) DAPI. (H) Fused imaged of panels F and G. Scale bar = 30 um.

Table

Inductively coupled plasma mass spectrometry (ICP-MS) 24 hours after the injection of Gd-TO.

Organ	%ID per g	%ID per organ
Heart *	0.0102 ± 0.0037	0.0012 ± 0.0004
Spleen	0.115 ± 0.0339	0.0091 ±0.0027
Stomach	0.0916 ± 0.0268	0.0291 ± 0.0085
Liver	2.74 ± 0.3809	2.63 ± 0.3655
Kidneys	0.784 ± 0.1739	0.206 ± 0.0457
Intestines	0.493 ± 0.3248	0.774 ± 0.5101
Lungs	0.0299 ± 0.0075	0.0040 ± 0.0001
Bone	0.0409 ± 0.0047	0.0819 ± 0.0094
Brain	<0.006	<0.002
Blood	<0.02	<0.03
Pancreas	<0.005	<0.0008

ID = injected dose.

* It should be noted that half the animals studied with ICP-MS had infarcts greater than 72 hours in duration at the time of Gd-TO injection.